Letter

Dynamical spacetimes from nonlinear perturbations

Karan Fernandes[1,2,*] Susovan Maity[2,†] and Tapas Das[2,3,‡]

[1]Department of Physics, National Taiwan University, Taipei 10617, Taiwan

[2]Harish-Chandra Research Institute, HBNI, Chhatnag Road, Jhusi, Allahabad 211019, India

[3]Homi Bhabha National Institute, Training School Complex, Anushakti Nagar, Mumbai 400094, India

(Received 14 February 2022; accepted 22 June 2022; published 28 July 2022)

Analog gravity describes fluctuations of hydrodynamic systems in terms of a massless scalar field propagating on curved spacetimes. This analogy between hydrodynamic and gravitational systems remains largely unexplored for nonlinear dynamical effects. In this paper, we provide the first description of dynamical analog spacetimes up to arbitrary order nonlinear perturbations constructed about stationary solutions. We find a high frequency response that exhibit known properties of perturbed black holes, as well as a low frequency regime for analog spacetimes with novel characteristics. Our framework more generally describes nonlinear perturbations of compressible hydrodynamic systems as analogs of nonlinear wave phenomena on black hole spacetimes.

DOI: 10.1103/PhysRevD.106.L021701

I. INTRODUCTION

Unruh established that fluctuations of inhomogeneous fluids can be described as a massless scalar field propagating on relativistic spacetimes constructed from the background flow [1]. This result forms the basis of the analog gravity programme, to investigate gravitational phenomena through hydrodynamical nongravitating systems [2–5]. An important class of analog solutions are dumb hole spacetimes, the acoustic analogs of black holes, that possess sonic horizon(s) from which phonons cannot escape. These solutions arise in fluids that transition from subsonic to supersonic flows, and are realized from condensed matter systems [6–18] to astrophysical accretion [19–29].

Analogue phenomena provide an experimental means to test black hole evaporation and evolution [30–33]. The analogs of Hawking radiation [34–39], quasinormal modes 40]] and superradiance [41] have been detected, confirming the analogy of dumb holes with black holes. Owing to the nonlinearity of hydrodynamics and gravitational systems, a more complete analogy will require a formalism for higher order perturbations. Several results for backreaction effects from second order perturbations about stationary analog spacetimes have been investigated [42–48], but were assumed to provide small corrections to linear order fluctuations. However, recent experiments have established that second and higher order perturbations provide observable late time effects. This includes the effect of second order fluctuations on the height over time in the draining bath tub model [48] and the spectrum of Hawking radiation through the lifetime of dumb holes in Bose-Einstein condensates [49]. To explain these effects, we require a framework for late time observables on dynamical analog spacetimes.

In this paper, we provide the first construction of dynamical analog spacetimes to all orders in perturbation about a stationary solution. This demonstrates that the analog paradigm is a more general phenomena than previously assumed. We address spherically symmetric, barotropic and inviscid fluids, that are compressible following nonlinear perturbations. Our approach makes use of the mass accretion rate as an independent variable, which characterizes the fluid's compressibility and is of particular importance in astrophysical accretion [50]. We show that the time derivative of the Euler equation, in terms of the fluid mass accretion rate and density, can be recast as a wave equation. The interpretation of fluctuations on a dynamical acoustic spacetime follows on expanding the fields about a stationary solution.

We consider the dynamics of dumb holes to find properties similar to perturbed black holes, as well as scenarios with a dynamically shrinking acoustic horizon. To explore these effects, we consider exponentially damped, time dependent perturbations of a Bondi flow accreting into a black hole. The perturbations are considered in "high" and "low" frequency regimes, which respectively involve wavelengths smaller than the inner radius and larger than the outer radius of the accreting fluid. The high frequency perturbations cause the dumb hole horizon to grow over time, analogous to black holes. However low frequency perturbations lead to a shrinking acoustic horizon, with no known black hole analog.

*karanfernandes@hri.res.in
†susovanmaity@hri.res.in
‡tapas@hri.res.in

II. SYSTEM

The equations for nonrelativistic and inviscid fluids are the continuity equation

$$\dot{\rho} + \vec{\nabla}(\rho\vec{v}) = 0, \tag{1}$$

and Euler equation

$$\dot{\vec{v}} + \vec{v}\,\vec{\nabla}\,\vec{v} + \frac{1}{\rho}\vec{\nabla}P + \vec{\nabla}\Phi = 0. \tag{2}$$

In these equations, overdots denote time derivatives and $\vec{\nabla}$ is the spatial derivative. The density, pressure, and velocity of the fluid are respectively denoted by ρ, P and $\vec{v}$, while Φ is the potential of an external force.

We will consider spherically symmetric and barotropic flows. The barotropic condition $P = P(\rho)$ allows us to define a scalar function $H(\rho)$ such that $\vec{\nabla}H = \frac{1}{\rho}\vec{\nabla}P$. With the sound speed c_s defined by $c_s^2 = \frac{\partial P}{\partial \rho}$, we find

$$\frac{\partial H}{\partial \rho} = \frac{c_s^2}{\rho}. \tag{3}$$

Spherical symmetry implies a spatial dependence on the radial distance and a nonvanishing radial velocity component, which we denote by v. While the fields also depend on time, we assume a time independent external potential $\Phi = \Phi(r)$. Hence Eqs. (1) and (2) simplify to the following two dimensional equations

$$\dot{\rho} + \frac{1}{r^2}(r^2\rho v)' = 0, \tag{4}$$

$$\dot{v} + vv' + H' + \Phi' = 0, \tag{5}$$

where primes now denote derivatives with respect to r in Eqs. (4) and (5). We define the mass accretion rate

$$f = \rho v r^2, \tag{6}$$

and consider the system in terms of f and ρ. In the case of Eq. (4) we find from direct substitution

$$\dot{\rho} + \frac{1}{r^2}f' = 0. \tag{7}$$

The time derivative of Eq. (5) can be shown to provide a wave equation. We first use Eqs. (6) and (7) to find

$$\dot{v} = \frac{1}{\rho r^2}\left(\dot{f} + \frac{f\partial_r f}{\rho r^2}\right). \tag{8}$$

From the expressions for $\frac{\partial H}{\partial \rho}$, v and $\dot{v}$ in Eqs. (3), (6), and (8) respectively, the time derivative of Eq. (5) yields the following second order equation

$$\partial_t\left(\frac{1}{\rho r^2}\partial_t f\right) + \partial_t\left(\frac{f}{\rho^2 r^4}\partial_r f\right) + \partial_r\left(\frac{f}{\rho^2 r^4}\partial_t f\right) + \partial_r\left(\left(\frac{f^2}{\rho^3 r^6} - \frac{c_s^2}{\rho r^2}\right)\partial_r f\right) = 0. \tag{9}$$

By defining the "inverse metric" components

$$g^{tt} = \frac{1}{\rho r^2}, \quad g^{rt} = \frac{f}{\rho^2 r^4} = g^{tr}, \quad g^{rr} = \frac{f^2}{\rho^3 r^6} - \frac{c_s^2}{\rho r^2}, \tag{10}$$

we find Eq. (9) takes the suggestive form

$$\partial_\mu(g^{\mu\nu}\partial_\nu f) = 0. \tag{11}$$

Equation (11) will describe fluctuations on a curved background only after perturbatively expanding about a stationary solution. The solutions of Eqs. (4) and (5) are generally not the same as those for Eqs. (7) and (11), since Eq. (11) results from a time derivative of Eq. (5). However, boundary conditions specify a unique stationary solution of Eqs. (4) and (5) that manifestly satisfy Eqs. (7) and (11). Subsequently, a perturbative solution for f from the original fluid equations will be one of the solutions of Eq. (11) through a consistently chosen boundary condition in time.

We can further express Eq. (11) as

$$\frac{1}{\sqrt{-G}}\partial_\mu(\sqrt{-G}G^{\mu\nu}\partial_\nu f) = 0. \tag{12}$$

For two dimensional flows, this is achieved by introducing additional spatial metric components, such as $g^{\theta\theta}$ and $g^{\phi\phi} = \frac{g^{\theta\theta}}{\sin\theta}$, that respect spherical symmetry without modifying Eq. (11). As this transformation does not affect the causal structure or dynamics, we will consider the unique two dimensional inverse effective metric $g^{\mu\nu}$ with components given in Eq. (10).

III. NONLINEAR PERTURBATIONS

The flow governed by Eqs. (7) and (11) can perturbatively solved about a spherically symmetric stationary solution, characterized by a constant mass accretion rate f_0 and a time independent density $\rho_0(r)$. In this case, an nth order expansion of $f(r,t)$ and $\rho(r,t)$ takes the form

$$f(r,t) = f_0 + \sum_{k=1}^{n}\epsilon^k f_k(r,t), \tag{13}$$

$$\rho(r,t) = \rho_0(r) + \sum_{k=1}^{n}\epsilon^k \rho_k(r,t), \tag{14}$$

where ϵ is a dimensionless counting parameter, whose power identifies the perturbation order. If a general field $A(r,t)$ constructed from ρ and f has the expansion

$$A(r,t) = A_0(r) + \sum_{k=1}^{n}\epsilon^k A_k(r,t), \tag{15}$$

then it is perturbative provided

$$\epsilon \frac{|A_{l+1}|}{|A_l|} < 1, \qquad l = 0, \qquad \cdots n-1. \tag{16}$$

The equations at order n are coefficients of ϵ^n on substituting Eqs. (13) and (14) in Eqs. (7) and (11), while the solutions are determined iteratively. The coefficients of ϵ^0 are identically satisfied by the stationary solution. From the terms linear in ϵ, Eqs. (7) and (11) give

$$\dot{\rho_1} + \frac{\partial_r f_1}{r^2} = 0, \qquad \partial_\mu (g^{\mu\nu}_{(0)} \partial_\nu f_1) = 0, \tag{17}$$

where $g^{\mu\nu}_{(0)}$ has the coefficients

$$g^{tt}_{(0)} = \frac{1}{\rho_0 r^2}, \; g^{tr}_{(0)} = \frac{f_0}{\rho_0^2 r^4} = g^{rt}_{(0)}, \; g^{rr}_{(0)} = \frac{f_0^2}{\rho_0^3 r^6} - \frac{c_{s0}^2}{\rho_0 r^2}. \tag{18}$$

The first order fluctuation $f_1(r,t)$ propagates on an acoustic background constructed entirely from the background flow. This agrees with known approaches to stationary analog spacetimes. We can solve Eq. (17) for $f_1(r,t)$ and subsequently for $\rho_1(r,t)$.

The ϵ^2 coefficients of Eqs. (7) and (11) are

$$\dot{\rho_2} + \frac{\partial_r f_2}{r^2} = 0, \tag{19}$$

$$\partial_\mu (g^{\mu\nu}_{(0)} \partial_\nu f_2) + \partial_\mu (g^{\mu\nu}_{(1)} \partial_\nu f_1) = 0, \tag{20}$$

with the $g^{\mu\nu}_{(1)}$ components

$$\begin{aligned} g^{tt}_{(1)} &= \frac{1}{r^2 \rho_0}\left(-\frac{\rho_1}{\rho_0}\right), \quad g^{tr}_{(1)} = \frac{f_0}{r^4 \rho_0^2}\left(\frac{f_1}{f_0} - 2\frac{\rho_1}{\rho_0}\right) = g^{rt}_{(1)}, \\ g^{rr}_{(1)} &= \frac{f_0^2}{r^6 \rho_0^3}\left(2\frac{f_1}{f_0} - 3\frac{\rho_1}{\rho_0}\right) - \frac{c_{s0}^2}{\rho_0 r^2}\left(\frac{\rho_1}{c_{s0}^2}\frac{\partial c_s^2}{\partial \rho}|_{\rho_0} - \frac{\rho_1}{\rho_0}\right), \end{aligned} \tag{21}$$

where $\frac{\partial c_s^2}{\partial \rho}|_{\rho_0}$ represents the derivative of c_s^2 with respect to ρ, evaluated at ρ_0. The usual procedure of first perturbing the system and then deriving the analog background would reproduce Eq. (20), which appears as a wave equation with an effective first order source. However, Eq. (11) informs us that Eq. (20) and $\partial_\mu (g^{\mu\nu}_{(0)} \partial_\nu f_1) = 0$ from Eq. (17) are collectively a second order fluctuation $f_0 + \epsilon f_1 + \epsilon^2 f_2$ propagating on an effective first order background with inverse metric $g^{\mu\nu}_{(0)} + \epsilon g^{\mu\nu}_{(1)}$.

The iterative procedure can be carried out to all orders. At order n we have the equations

$$\dot{\rho_n} = -\frac{\partial_r f_n}{r^2}, \tag{22}$$

$$\partial_\mu (g^{\mu\nu}_{(0)} \partial_\nu f_n) = -\sum_{k=1}^{n-1} \partial_\mu (g^{\mu\nu}_{(k)} \partial_\nu f_{n-k}). \tag{23}$$

The nth order fluctuation $f_0 + \cdots + \epsilon^n f_n$ propagates on an effective $(n-1)$th order background with inverse metric

$$g^{\mu\nu}_{\mathrm{eff}(n-1)} = \sum_{k=0}^{n-1} \epsilon^k g^{\mu\nu}_{(k)}. \tag{24}$$

IV. HORIZON VARIATIONS

The inverse metric to all orders can be compactly represented using Eq. (10), with the order n expression resulting from Eq. (24). Inverting Eq. (10) provides the following acoustic metric

$$\begin{aligned} g_{\mu\nu} &= \begin{pmatrix} g_{tt} & g_{tr} \\ g_{rt} & g_{rr} \end{pmatrix} = \begin{pmatrix} gg^{rr} & -gg^{rt} \\ -gg^{tr} & gg^{tt} \end{pmatrix} \\ &= \begin{pmatrix} \rho r^2(1-\beta^2) & \frac{f}{c_s^2} \\ \frac{f}{c_s^2} & -\frac{\rho r^2}{c_s^2} \end{pmatrix}, \end{aligned} \tag{25}$$

where $g = -\frac{\rho^2 r^4}{c_s^2}$ is the determinant of the metric and $\beta = \frac{f}{c_s \rho r^2}$ is the fluid velocity to sound speed ratio. In units with the speed of light $c = 1$, we have $0 < v = \frac{f}{\rho r^2} < 1$ and $0 < \beta < \frac{1}{c_s}$. The condition $g_{tt} = 0$, or equivalently $g^{rr} = 0$, determines the horizon radius r_H

$$r_H^4 = \frac{f^2}{\rho^2 c_s^2}. \tag{26}$$

The variation of Eq. (26) gives the acoustic horizon change from any perturbation order to the next

$$\frac{\delta r_H}{r_H} = \frac{1}{2}\frac{\delta f}{f} - \frac{1}{4}\frac{\delta \rho}{\rho}\left(\frac{1}{c_s^2}\frac{\partial c_s^2}{\partial \rho}|_\rho + 2\right). \tag{27}$$

Here ρ, f and r_H denote values at a specific order in perturbation, while $\delta\rho$, δf and δr_H describe their relative variations to the next order. Using Eq. (7), we deduce

$$\frac{\delta f}{f} = \frac{\int dr r^2 \delta\dot{\rho}}{\int dr r^2 \dot{\rho}}. \tag{28}$$

The relative mass accretion rate change $\frac{\delta f}{f}$ is thus related to a spatially averaged change in energy and is expected to be positive. The relative density change $\frac{\delta \rho}{\rho}$ however is not constrained. In particular, if it is positive and greater than $\frac{\delta f}{f}$, Eq. (27) admits a receding acoustic horizon.

V. SIMULATION

We consider the example of a spherically symmetric adiabatic flow satisfying the isentropic condition $P = \kappa\rho^\gamma$, accreting due to a Newtonian potential $\Phi = -\frac{1}{r}$. The sound speed is $c_s^2 = \kappa\gamma\rho^{\gamma-1}$. Bondi demonstrated that there exists a unique transonic solution of Eqs. (4) and (5) which passes through a critical point $v_0(r) = c_{s0}(r)$ [51]. The solution can be derived by specifying γ, κ and the Bernoulli constant

$$\mathcal{E}_0 = \frac{v_0^2}{2} + \frac{c_{s0}^2}{\gamma - 1} + \Phi. \tag{29}$$

We assume $\gamma = 1.35$, $\kappa = 1$ and $\mathcal{E}_0 = 1.001$. With the accretor taken to be a black hole, the fluid velocity can approach close to the speed of light ($v = 1$) at the inner radius. The background solution plots are in the top panel of Fig. 1, with further details in [52]. The solution has a mass accretion rate $f_0 = 0.0129$. Using the $\rho_0(r)$, $c_{s0}(r)$ and f_0 solutions, we find the lowest order inverse acoustic metric components plotted in the bottom panel of Fig. 1, with the acoustic horizon at $r_H = 2.362$.

We now consider exponentially damped in time $e^{-\omega t}$ perturbations. The accreting fluid has an outer boundary at $r = 10^2$ and an inner boundary at $r = 1.002$ near the accretor. The boundary conditions at initial time ($t = 0$) are chosen to agree with the preceding perturbation order, i.e., $f_{l+1}(r, 0) = f_l(r, 0)$ and $\rho_{l+1}(r, 0) = \rho_l(r, 0)$ for $l = 1, \cdots n$. We additionally fix $\rho(10^2, t)$ for all times to match the stationary solution. The perturbation introduced at $t = 0$ is considered up to $t = 10^3$, an order of magnitude larger than the spatial range. This ensures that a perturbative damping up to late times. The inner and outer spatial boundaries allow us to consider two frequency ranges. "High frequency" perturbations $\omega_{\rm high} \geq 1$ involve wavelengths that are the size of the accretor boundary or lower, while "Low frequency" perturbations $\omega_{\rm low} \leq 10^{-2}$ involve wavelengths larger than the outer boundary radius. We will set $\omega_{\rm high} = 10^3$ and $\omega_{\rm low} = 10^{-3}$. In all cases, the first order metric solution for $g^{rr}_{(1)}$ has the largest amplitude among the inverse metric components, at a time $t = t_m$ and $r = 1.002$. We use this in Eq. (16) to fix the perturbation strength ϵ to 0.3

$$\epsilon \frac{|g^{rr}_{(1)}|_{(r=1.002, t=t_m)}}{|g^{rr}_{(0)}|_{(r=1.002)}} := 0.3. \tag{30}$$

The linear fluctuations are plotted in Fig. 2. In both high and low frequency cases, the fluctuations f_1 about the background acoustic spacetime involve growing and decaying modes in the subsonic region, with an increasing amplitude away from the horizon. This is a generic property of subsonic mass accretion rate fluctuations noted previously for traveling wave solutions [53]. In the supersonic region, only ingoing modes propagate and the averaged mass accretion rate increases. This agrees with our expectations following Eq. (28).

The density fluctuation ρ_1 differs in the high and low frequency cases. This fluctuation is negligible in the subsonic region of the background flow. Near the accretor boundary ρ_1 is negative in the high frequency case, while large and positive in the low frequency case. The negative density fluctuations in the supersonic region for high frequency perturbations causes the acoustic horizon to grow from $r_H(t = 0) = 2.362$ to $r_H(t = 10^3) = 2.468$. Conversely, positive density fluctuations in the low frequency case results in the horizon receding to $r_H(t = 10^3) = 2.213$. While a larger acoustic horizon at late times is consistent with the perturbations of black holes, a receding acoustic horizon under classical

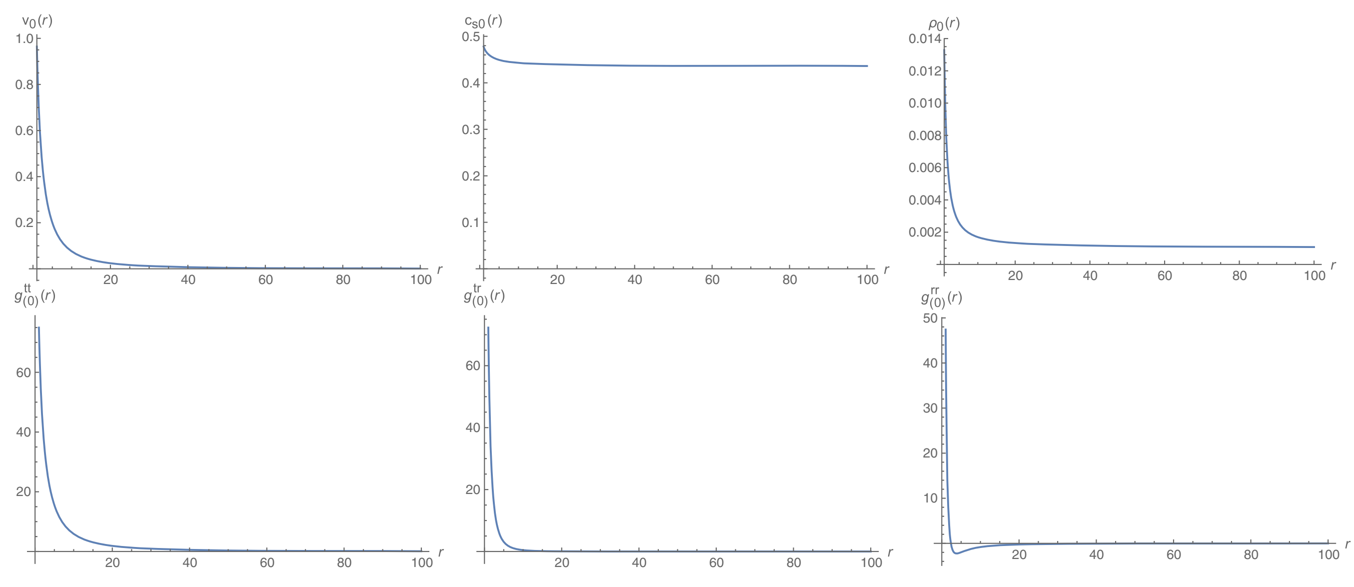

FIG. 1. The origin is at $(t, r) = (0, 1)$ in all plots. The top panels are solutions for $v_0(r)$ (left), $c_{s0}(r)$ (middle) and $\rho_0(r)$ (right), with $f_0 = 0.0129$. These solutions define the inverse acoustic metric components $g^{\mu\nu}_{(0)}$ plotted in the bottom panels: $g^{tt}_{(0)}(r)$ (left), $g^{tr}_{(0)}(r)$ (middle) and $g^{rr}_{(0)}(r)$ (right). We find $g^{rr}_{(0)} = 0$ at $r = 2.362$.

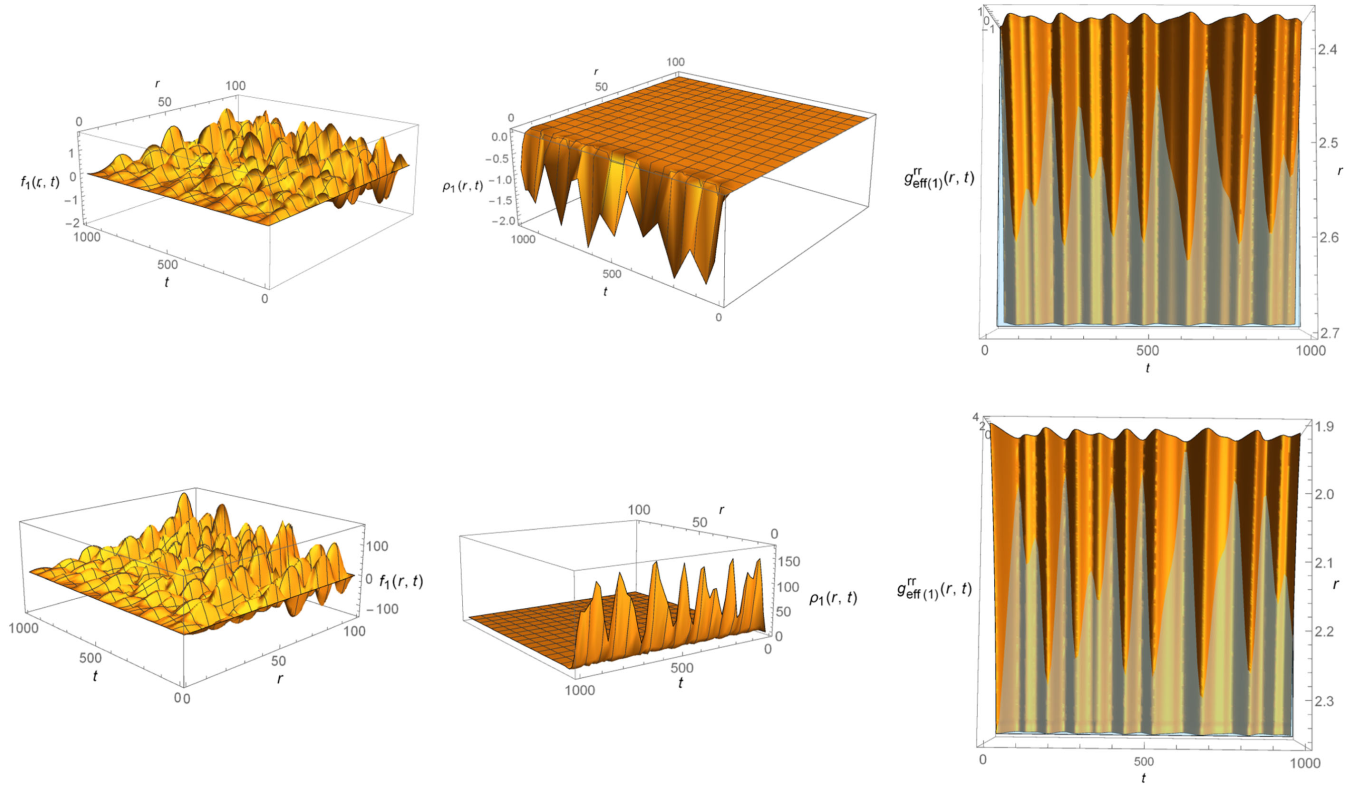

FIG. 2. Linearized perturbation results. With high frequency, f_1 interferes destructively outside the horizon and constructively within (top left), while ρ_1 is negative close to the accretor (top middle). With low frequency, f_1 behaves as in the high frequency case (bottom left), while ρ_1 is positive close to the accretor (bottom middle). The horizon evolution is considered by plotting g^{rr} close to the horizon at $t = 0$, with the blue plane $g^{rr} = 0$ tracing the horizon over time. The horizon grows from $r_H(t = 0) = 2.362$ to $r_H(t = 10^3) = 2.468$ in the high frequency case (top right) and shrinks from $r_H(t = 0) = 2.362$ to $r_H(t = 10^3) = 2.213$ in the low frequency case (bottom right).

perturbations has no known black hole analog. This is a consequence of there being no low energy cut off for gravitational theories on asymptotically flat spacetimes, while finite sized hydrodynamic systems do possess one.

Higher order fluctuations support the low frequency receding horizon effect. The second order solutions and qualitative properties at higher orders are presented in [52]. To higher perturbation orders, fluctuations in both high and low frequency regimes are qualitatively those of first order high frequency fluctuations. This has the effect of causing the acoustic horizon to grow and prevents an indefinite shrinking of the horizon. However, we find effective dynamical metric corrections that are suppressed by ϵ^n at order n. This leads to a horizon for the dynamical acoustic spacetime that does not recover its original size and which is well approximated by the first order effective metric.

VI. CONCLUSION

We provided a complete dynamical description of analog spacetimes consistent with all nonlinearities in the fluid equations for spherically symmetric, inviscid and nonrelativistic flows perturbed about a stationary solution. This result is a consequence of considering the system in terms of its mass accretion rate and density. We also identified a new property of classically receding acoustic horizons that occurs when the change in density fluctuation from a perturbation order to the next is positive and greater than the corresponding change in the mass accretion rate fluctuation. For exponentially damped Bondi accretion flows, this scenario is realized for perturbation wavelengths larger than the fluid.

It will be interesting to derive dynamical extensions of known analog spacetimes through our approach. This requires relating the analog spacetimes in our formalism with those from the standard approach based on velocity perturbations of general background flows with possibly time dependent potentials. Since mass accretion rates can be defined with respect to all velocity components, we believe that our formalism is likewise applicable to general flows with the mass accretion rate encoding properties of the velocity and background potential. The resulting wave equation and acoustic spacetime interpretation however depend on details of the flow and hence require a separate analysis that we intend to address in future work. We anticipate time dependent backgrounds and potentials to manifest in sourced wave equations, and additional wave equations in nonradial flows for each mass accretion rate defined with respect to the velocity components.

Wave equations for linearized mass accretion rate fluctuations determine the stability of flows, with solutions providing dispersion relations [53]. We expect modified dispersion relations from higher order fluctuations, which along with late time observables, could provide tests of our formalism in analog experiments [54].

ACKNOWLEDGMENTS

K. F. is supported by the Ministry of Science and Technology (MOST), Taiwan and would like to thank National Taiwan Normal University, National Taiwan University, and Harish-Chandra Research Institute for their hospitality during the completion of this work.

[1] W. Unruh, Experimental Black Hole Evaporation, Phys. Rev. Lett. **46**, 1351 (1981).
[2] M. Novello, M. Visser, and G. Volovik, *Artificial Black Holes* (World Scientific, Singapore, 2002).
[3] *Quantum Analogues: From Phase Transitions to Black Holes and Cosmology*, edited by W. Unruh and R. Schützhold (Springer, Berlin, 2007).
[4] C. Barcelo, S. Liberati, and M. Visser, Analogue gravity, Living Rev. Relativity **14**, 3 (2011); **8**, 12 (2005).
[5] D. Faccio, F. Belgiorno, S. Cacciatori, V. Gorini, S. Liberati, and U. Moschella, Analogue gravity phenomenology, Lect. Notes Phys. **870**, 1 (2013).
[6] L. J. Garay, J. R. Anglin, J. I. Cirac, and P. Zoller, Sonic Analog of Gravitational Black Holes in Bose-Einstein Condensates, Phys. Rev. Lett. **85**, 4643 (2000).
[7] L. J. Garay, J. R. Anglin, J. I. Cirac, and P. Zoller, Sonic black holes in dilute Bose-Einstein condensates, Phys. Rev. A **63**, 023611 (2001).
[8] C. Barcelo, S. Liberati, and M. Visser, Analog gravity from Bose-Einstein condensates, Classical Quantum Gravity **18**, 1137 (2001).
[9] C. Barcelo, S. Liberati, and M. Visser, Probing semiclassical analog gravity in Bose-Einstein condensates with widely tunable interactions, Phys. Rev. A **68**, 053613 (2003).
[10] T. A. Jacobson and G. E. Volovik, Effective spacetime and Hawking radiation from moving domain wall in thin film of He-3-A, JETP Lett. **68**, 874 (1998).
[11] G. E. Volovik, Simulation of Panlevé-Gullstrand black hole in thin He-3—A film, JETP Lett. **69**, 705 (1999).
[12] G. E. Volovik, Superfluid analogies of cosmological phenomena, Phys. Rep. **351**, 195 (2001).
[13] G. E. Volovik, Black-hole horizon and metric singularity at the brane separating two sliding superfluids, Pis'ma Zh. Eksp. Teor. Fiz. **76**, 296 (2002).
[14] S. Corley and T. Jacobson, Black hole lasers, Phys. Rev. D **59**, 124011 (1999).
[15] U. Leonhardt and P. Piwnicki, Relativistic Effects of Light in Moving Media with Extremely Low Group Velocity, Phys. Rev. Lett. **84**, 822 (2000).
[16] U. Leonhardt, Space-time geometry of quantum dielectrics, Phys. Rev. A **62**, 012111 (2000).
[17] R. Schutzhold and W. G. Unruh, Hawking Radiation in an Electromagnetic Waveguide?, Phys. Rev. Lett. **95**, 031301 (2005).
[18] T. G. Philbin, C. Kuklewicz, S. Robertson, S. Hill, F. Konig, and U. Leonhardt, Fiber-optical analogue of the event horizon, Science **319**, 1367 (2008).
[19] T. K. Das, Behavior of matter close to the event horizon, Mon. Not. R. Astron. Soc. **349**, 375 (2004).
[20] H. Abraham, N. Bilic, and T. K. Das, Acoustic horizons in axially symmetric relativistic accretion, Classical Quantum Gravity **23**, 2371 (2006).
[21] T. K. Das, N. Bilic, and S. Dasgupta, A black-hole accretion disc as an analogue gravity model, J. Cosmol. Astropart. Phys. 06 (2007) 009.
[22] N. Bilić, A. Choudhary, T. K. Das, and S. Nag, The role of axisymmetric flow configuration in the estimation of the analogue surface gravity and related Hawking like temperature, Classical Quantum Gravity **31**, 035002 (2014).
[23] P. Tarafdar, T. K. Das, and A. S. Majumdar, Dependence of acoustic surface gravity on geometric configuration of matter for axially symmetric background flows in the Schwarzschild metric, Int. J. Mod. Phys. D **24**, 1550096 (2015).
[24] M. A. Shaikh, I. Firdousi, and T. K. Das, Relativistic sonic geometry for isothermal accretion in the Schwarzschild metric, Classical Quantum Gravity **34**, 155008 (2017).
[25] M. A. Shaikh, Relativistic sonic geometry for isothermal accretion in the Kerr metric, Classical Quantum Gravity **35**, 055002 (2018).
[26] H. Y. Pu, I. Maity, T. K. Das, and H. K. Chang, On spin dependence of relativistic acoustic geometry, Classical Quantum Gravity **29**, 245020 (2012).
[27] S. Saha, S. Sen, S. Nag, S. Raychowdhury, and T. K. Das, Model dependence of the multi-transonic behaviour, stability properties and the corresponding acoustic geometry for accretion onto rotating black holes, New Astron. **43**, 10 (2016).
[28] P. Tarafdar and T. K. Das, Influence of the geometric configuration of accretion flow on the black hole spin dependence of relativistic acoustic geometry, Int. J. Mod. Phys. D **27**, 1850023 (2018).
[29] M. A. Shaikh and T. K. Das, Linear perturbations of low angular momentum accretion flow in the Kerr metric and the corresponding emergent gravity phenomena, Phys. Rev. D **98**, 123022 (2018).
[30] T. Jacobson, Black-hole evaporation and ultrashort distances, Phys. Rev. D **44**, 1731 (1991).
[31] S. Corley and T. Jacobson, Hawking spectrum and high frequency dispersion, Phys. Rev. D **54**, 1568 (1996).

[32] W. G. Unruh, Sonic analog of black holes and the effects of high frequencies on black hole evaporation, Phys. Rev. D **51**, 2827 (1995).
[33] W. G. Unruh and R. Schutzhold, Universality of the Hawking effect, Phys. Rev. D **71**, 024028 (2005).
[34] S. Weinfurtner, E. W. Tedford, M. C. J. Penrice, W. G. Unruh, and G. A. Lawrence, Measurement of Stimulated Hawking Emission in an Analogue System, Phys. Rev. Lett. **106**, 021302 (2011).
[35] J. Steinhauer, Observation of self-amplifying Hawking radiation in an analog black hole laser, Nat. Phys. **10**, 864 (2014).
[36] J. Drori, Y. Rosenberg, D. Bermudez, Y. Silberberg, and U. Leonhardt, Observation of Stimulated Hawking Radiation in an Optical Analogue, Phys. Rev. Lett. **122**, 010404 (2019).
[37] O. Lahav, A. Itah, A. Blumkin, C. Gordon, S. Rinott, A. Zayats, and J. Steinhauer, Realization of a Sonic Black Hole Analog in a Bose-Einstein Condensate, Phys. Rev. Lett. **105**, 240401 (2010).
[38] J. R. Muñoz de Nova, K. Golubkov, V. I. Kolobov, and J. Steinhauer, Observation of thermal Hawking radiation and its temperature in an analogue black hole, Nature (London) **569**, 688 (2019).
[39] J. Steinhauer, Observation of quantum Hawking radiation and its entanglement in an analogue black hole, Nat. Phys. **12**, 959 (2016).
[40] T. Torres, S. Patrick, M. Richartz, and S. Weinfurtner, Quasinormal Mode Oscillations in an Analogue Black Hole Experiment, Phys. Rev. Lett. **125**, 011301 (2020).
[41] T. Torres, S. Patrick, A. Coutant, M. Richartz, E. W. Tedford, and S. Weinfurtner, Rotational superradiant scattering in a vortex flow, Nat. Phys. **13**, 833 (2017).
[42] R. Balbinot, S. Fagnocchi, A. Fabbri, and G. P. Procopio, Backreaction in Acoustic Black Holes, Phys. Rev. Lett. **94**, 161302 (2005).
[43] R. Schutzhold, M. Uhlmann, Y. Xu, and U. R. Fischer, Quantum backreaction in dilute Bose-Einstein condensates, Phys. Rev. D **72**, 105005 (2005).
[44] R. Balbinot, A. Fabbri, S. Fagnocchi, and R. Parentani, Hawking radiation from acoustic black holes, short distance and backreaction effects, Riv. Nuovo Cimento **28**, 1 (2005).
[45] R. Balbinot, A. Fabbri, S. Fagnocchi, and A. Nagar, Numerical analysis of backreaction in acoustic black holes, Nuovo Cimento Soc. Ital. Fis. **121B**, 201 (2006).
[46] C. Maia and R. Schutzhold, Quantum toy model for black-hole backreaction, Phys. Rev. D **76**, 101502 (2007).
[47] S. Liberati, G. Tricella, and A. Trombettoni, Back-reaction in canonical analogue black holes, Appl. Sci. **10**, 8868 (2020).
[48] S. Patrick, H. Goodhew, C. Gooding, and S. Weinfurtner, Backreaction in an Analogue Black Hole Experiment, Phys. Rev. Lett. **126**, 041105 (2021).
[49] V. I. Kolobov, K. Golubkov, J. R. Muñoz de Nova, and J. Steinhauer, Observation of stationary spontaneous Hawking radiation and the time evolution of an analogue black hole, Nat. Phys. **17**, 362 (2021).
[50] J. Frank, A. King, and D. J. Raine, *Accretion Power in Astrophysics*, 3rd ed. (Cambridge University Press, Cambridge, England, 2002).
[51] H. Bondi, On spherically symmetrical accretion, Mon. Not. R. Astron. Soc. **112**, 195 (1952).
[52] K. Fernandes, S. Maity, and T. Das, following paper, Dynamical analog spacetimes in nonrelativistic flows, Phys. Rev. D **106**, 025020 (2022).
[53] J. A. Petterson, J. Silk, and J. P. Ostriker, Variations on a spherically symmetrical accretion flow, Mon. Not. R. Astron. Soc. **191**, 571 (1980).
[54] M. J. Jacquet, S. Weinfurtner, and F. König, The next generation of analogue gravity experiments, Phil. Trans. R. Soc. A **378**, 20190239 (2020).